



Research Article

Flip-flop states in X-ray binaries and changing-state AGN

Thomas Maccarone¹, Jessie C Runnoe², Gregoire Marcel³, Emilia Järvelä¹, Douglas Buisson⁴, Unnati Kashyap¹ and Federico Vincentelli^{5,6,7}

¹Department of Physics & Astronomy, Texas Tech University, Lubbock, TX, USA, ²Department of Physics & Astronomy, Vanderbilt University, Nashville, TN, USA, ³Department of Physics and Astronomy, University of Turku, Finland, ⁴Independent Scientist, UK, ⁵Fluid and Complex Systems Centre, Coventry University, Coventry, UK, ⁶INAF—Istituto di Astrofisica e Planetologia Spaziali, Roma, Italy and ⁷School of Physics & Astronomy, University of Southampton, Southampton, UK

Abstract

We show that the flip-flop transitions in X-ray binaries (rapid cycling between different spectral states which are sometimes seen near the global state transition) show a series of analogies to the changing state phenomena (rapid changes in the emission line properties that seem to be driven by changes in the central engine) in active galactic nuclei (AGN). Specifically, (1) the timescales for the transitions scale approximately linearly with mass and (2) both phenomena occur at a few percent of the Eddington luminosity. Because most accretion physics is expected to be scale-free, it is likely that these represent two manifestations of the same phenomena. Demonstrating this would allow the use of a much wider range of observational techniques, on a much wider range of characteristic timescales, and provide a clearer pathway towards understanding these rapid transitions than is currently available. We discuss potential means to establish the connection more firmly and to use the combination of the observational advantages of both classes of systems to develop a better understanding of the phenomenon.

Keywords: Galaxies: active; black hole physics; accretion; accretion discs; X-rays: binaries

(Received 4 December 2025; revised 25 February 2026; accepted 6 March 2026)

1. Introduction

Black hole accretion is a fundamentally important astrophysical process. On the supermassive scale, it powers active galactic nuclei, which are one of the main sources of energetic feedback that affects cosmological structure formation (Fabian 2012). On the stellar mass side, it also provides the means for identifying stellar mass black holes in environments where their spins can be estimated, giving clues to the nature of the supernova explosion mechanism that cannot be achieved any other way (Fryer et al. 2012). In both cases, these systems may also be outstanding particle accelerators, producing high-energy photons (Punch et al. 1992; Tavani et al. 2009), neutrinos (IceCube Collaboration et al. 2018; Koljonen et al. 2023), and cosmic rays (Heinz & Sunyaev 2002; Pierre Auger Collaboration et al. 2007).

Most phenomena related to black hole accretion are expected to be relatively scale-free, in the sense that accretion geometry and kinetic power into the jet will depend primarily on the accretion rate scaled to the black hole mass; only a few aspects of black hole accretion have strong dependencies on the density and temperature of the accretion flow because it affects the atomic physics equilibria. Indeed, past work has shown many analogies in the behaviour of black hole X-ray binaries and AGN. For example, it was first seen in X-ray binaries that there are some sharp transitions in their X-ray spectral and timing behaviours that can set on

relatively quickly, indicative of a fundamental change of the geometry of the accretion flow (Tananbaum et al. 1972). Evidence for spectral states similar to those of stellar mass black holes appears in power spectra (McHardy et al. 2006), jet power (Tananbaum et al. 1972; Merloni, Heinz, & di Matteo 2003; Maccarone, Gallo, & Fender 2003), and spectral energy distributions (Tananbaum et al. 1972; Ho 1999; Trichas et al. 2013), and the transition between phenomenology similar to that in the hard state and similar to that in the soft state occurs at luminosities close to 2% of the Eddington limit in both X-ray binaries (Maccarone 2003; Vahdat Motlagh, Kalemci, & Maccarone 2019) and AGN (Maccarone et al. 2003; Körding, Jester, & Fender 2006; Moravec et al. 2022).

For studies of accretion physics, stellar mass and supermassive black holes provide highly complementary data. For most purposes, stellar mass black holes, with their much higher signal-to-noise, can be studied in greater detail. Their black hole masses are more straightforward to measure, at least in the cases of transients with bright donor stars. Because of their smaller masses and faster characteristic timescales, black holes in transient accretion discs can vary by factors of millions within years, allowing a system with a constant mass and spin to be studied over a wide range of accretion rates. Additionally, because of their higher disc temperatures, they are closer to fully ionised, making the physics of their accretion discs simpler to understand. Such studies of stellar mass black holes can then inform the best way to assemble samples of AGN to probe their accretion physics.

Supermassive black holes have a few key advantages, as well. In particular, for certain purposes, their longer characteristic timescales are a benefit. In supermassive black holes, phenomena happening on thermal, and even dynamical, timescales can be

Corresponding author: Thomas Maccarone; Email: thomas.maccarone@ttu.edu

Cite this article: Maccarone T, Runnoe JC, Marcel G, Järvelä E, Buisson D, Kashyap U and Vincentelli F. (2026) Flip-flop states in X-ray binaries and changing-state AGN. *Publications of the Astronomical Society of Australia* 43, e044, 1–9. <https://doi.org/10.1017/pasa.2026.10176>

Table 1. (Top) Theoretical disc timescales at $R = 10 R_g$ assuming $\alpha = 0.1$ and $H/R = 0.1$. (Bottom) Observed characteristic timescales of stellar-mass black hole transitions and their mass-scaled AGN equivalents (assuming $t \propto M$).

Disc timescales	$10 M_\odot$	$10^7 M_\odot$	$10^{10} M_\odot$
$t_{\text{dyn}} = \Omega_K^{-1}$	1.6 ms	26 min	18 d
$t_{\text{th}} = \alpha^{-1} t_{\text{dyn}}$	16 ms	4.3 h	181 d
$t_{\text{visc}} = \alpha^{-1} (H/R)^{-2} t_{\text{dyn}}$	1.6 s	18 d	49 yr
State timescales	$10 M_\odot$	$10^7 M_\odot$	$10^{10} M_\odot$
X-ray state transitions	$\gtrsim 1$ week	$\gtrsim 20$ kyr	$\gtrsim 200$ Myr
Flip-flop state transition	s to hours	wks to centuries	30 yr to Myr

seen directly evolving. In stellar mass black holes, these phenomena can often be studied only statistically, via Fourier methods. In particular, stellar mass black holes typically show count rates of a few thousand counts per second, with dynamical timescales of a few milliseconds, yielding of order 1–10 photons per dynamical timescale with high collecting area facilities like the Rossi X-ray Timing Explorer and Neutron star Interior Composition Explorer (NICER). The nearest bright AGN show count rates a few orders of magnitude smaller, but with characteristic timescales about 5–7 orders of magnitude longer, so that there are often thousands of counts per dynamical timescale. The fastest variability, in units of the dynamical timescale, is thus best probed in AGN (e.g. McHardy *et al.* 2006). Fourier methods do allow compensating for the lack of photons per characteristic timescales in the stellar mass black holes by making statistical studies possible over large numbers of characteristic timescales. Table 1 shows some characteristic timescales for accretion discs around different black hole masses.

Additionally, supermassive black hole accretion discs emit more of their power in the optical band. Because optical telescopes are far more sensitive in flux units than X-ray telescopes, they allow the discovery and time-domain monitoring of a much larger number of AGN than of stellar mass black holes (e.g. Rumbaugh *et al.* 2018; Komossa & Grupe 2024). This can even include spectroscopic monitoring (Dong *et al.* 2025b). As a result, intrinsically rapid variability can be discovered in AGN from survey data, while in stellar mass black holes, it can generally only be discovered in pointed observations.

One of the key findings from studies of stellar mass black holes is that they show a set of states in which spectral properties, variability properties, and relativistic jet power are strongly correlated. The ‘hard state’ is characterised by a $\Gamma = 1.5$ –1.8 power law with a rollover around 100 keV (along with a weak thermal accretion disc peaking below 1 keV), broadband variability with a root mean square (rms) amplitude of up to about 30% (van der Klis 1994), and with strong radio emission that usually follows a $L_R \propto L_X^{0.7}$ relation (Hannikainen *et al.* 1998; Gallo, Fender, & Pooley 2003). The soft states have properties that agree well with the predictions of the Shakura-Sunyaev disc model, and are well-matched spectrally as sums of blackbodies with $T \propto R^{-3/4}$ (Zhang, Cui, & Chen 1997), and show little to no variability, and generally show no radio emission (Tananbaum *et al.* 1972; Maccarone *et al.* 2020). Intermediate states show a rather complicated phenomenology, with spectra that generally have strong thermal and strong non-thermal components, and power spectra that show strong quasi-periodic oscillations (QPOs, see, e.g. Motch *et al.* 1983; Homan *et al.* 2001).

In recent years, both the X-ray binaries and the AGN have shown some examples of objects that change spectral appearances

very quickly. In the X-ray binaries, these changes are known as flip-flop transitions (Takizawa *et al.* 1997). In the AGN, the objects are called changing-look AGN (Ricci & Trakhtenbrot 2023). In this paper, we discuss the broad similarities of the two phenomena, and discuss potential observational tests that could be used to determine if they are, indeed, two manifestations of the same process, on different mass scales.

2. Properties of flip-flop transitions

The first clear example of flip-flop transitions in X-ray binaries was GX 339-4 (Miyamoto *et al.* 1991). In these observations, the source count rate alternates between two distinct levels, differing by only a few percent. These transitions occur on timescales of seconds, yet a given state can persist for hours. In conjunction with these changes, flip-flops see the variability shift between two markedly different regimes (typically between cases dominated by a single QPO and cases dominated by broadband aperiodic variability). For a comprehensive summary of the literature on this topic, we refer the reader to the introduction of Buisson *et al.* (2025).

The flip-flop transitions can be seen both in hard-to-soft state transitions, and in soft-to-hard transitions (Buisson *et al.* 2025). These generally occur at somewhat different Eddington fractions, because of hysteresis in state transition luminosities (Miyamoto *et al.* 1991; Maccarone & Coppi 2003). It is likely that if changing-state AGN (CSAGN) are the analogs of flip-flop transitions, and AGN follow the same outburst phenomenology with hysteresis effects (Körding *et al.* 2006) that the CSAGN will be seen mostly during the slower, fainter soft-to-hard state transitions, simply because those last longer.

Normally, state transitions are thought to be driven by changes in accretion rate. The viscous timescale, t_{visc} , in an accretion disc is thought to be the fastest timescale on which the accretion rate can vary substantially. It is given by:

$$t_{\text{visc}} = \alpha^{-1} \left(\frac{H}{R} \right)^{-2} t_{\text{dyn}}, \quad (1)$$

where α is the dimensionless viscosity parameter, H is the vertical height of the disc, R is the radial scale of the disc for which the timescale is calculated, and t_{dyn} is the dynamical timescale, which is the Keplerian orbital period.

For typical parameters for X-ray binaries in states dominated by geometrically thin components, this timescale will be typically a few seconds or more (although if a very small region mediates the state changes, the viscous timescale across that region may be small – Sniegowska *et al.* 2020). The flip-flop transitions thus set on with timescales much faster than the local viscous timescale, indicating that they are *not* likely due to fundamental changes in the mass transfer rate; in particular because one typically expects variations in accretion rate to be driven by the outer regions, where t_{visc} is of the order of hours. Also in agreement with this is that there are no large changes in the bolometric luminosity across the flip-flop transitions.

An alternative timescale of interest is the thermal timescale, t_{th} (see e.g. Bogensberger *et al.* 2020). This is given by:

$$t_{\text{th}} = \alpha^{-1} t_{\text{dyn}} \quad (2)$$

Contrarily to the (local) viscous timescale, this thermal timescale can be around or below a second, i.e. the right order of magnitude for spectral changes observed during flip-flops of X-ray binaries (Buisson *et al.* 2025).

3. Properties of changing look AGN

Ricci & Trakhtenbrot (2023) give a recent review of the details of changing-look AGN (CLAGN). They appear to be a heterogeneous class, with a subset of CLAGN caused by changing absorption, and the remainder being due to some fundamental change in the accretion process. These are sometimes classified in a manner that distinguishes between changing obscuration and changing state.

In a substantial sample of objects, there is strong evidence for a pattern in which the CSAGN behave in a manner similar to changes of states in X-ray binaries. Specifically, the UV to X-ray spectral slopes change at Eddington fractions similar to those for the X-ray binaries (Noda & Done 2018; Ruan et al. 2019; Panda & Śniegowska 2024). Samples of steadier AGN also show phenomenology indicative of spectral states changing at such Eddington fractions (Maccarone et al. 2003; Sobolewska, Siemiginowska, & Gierliński 2011). In several cases, there is even clearer evidence that a change in accretion disc intrinsic properties, rather than a change in absorption must be responsible for the changes in CSAGN (Duffy et al. 2025b). The observed spectral changes are more dramatic than for the X-ray binaries, but this is likely because in AGN the thermal disc emission is in the optical-through-UV range, well separated from the Compton scattering emission.

The characteristic timescales for the CSAGN (Table 1) appear to be roughly consistent with what would be expected from scaling up the stellar mass black holes' flip-flop oscillations, based on a few objects seen to return from faint states to bright ones (Duffy et al. 2025a; Dong et al. 2025a). The source SDSS J101152.98+544206.4 took about 500 d to make its state transitions, and stayed in a faint state for about 10.6 yr. Given its black hole mass of $10^{7.6} M_{\odot}$, assuming a linear scaling of key timescales with mass, this corresponds to an ingress time of a few seconds for a stellar mass black hole and a faint state duration of about a minute (Duffy et al. 2025a); Mrk 1018, which has a black hole mass a factor of about three higher had a bright state a factor of about three longer (Dunn et al. 2025). The two other sources in Duffy et al. (2025a), both of which showed the same phenomenology of returning to bright states, were less well sampled and have larger mass black holes, but are broadly consistent with the same timescales. In a larger sample of objects with LAMOST spectroscopy, about 10% of objects showed recurring changes, with typical observed recurrence times of a few years (Dong et al. 2025a). Here, again with relatively sparse sampling meaning that it is likely that many objects had missed transitions, so that some recurrence times may be faster than a few years, and a higher percentage of objects likely show recurring changes within timescales of a few years. In comparison, Buisson et al. (2025) finds state changes with typical durations of tens of seconds in X-ray binaries (see e.g. their Figure 6). Better sampling of more AGN is needed to develop conclusive evidence that these timescales are proportional to black hole mass, but the existing evidence is strongly suggestive of this.

4. Potential tests and applications of the scenario

Broad similarities exist between the flip-flop state transitions in X-ray binaries and the CSAGN transitions. Specifically, (1) the characteristic timescales of the ingresses, egresses, and durations of the states generally are consistent with being linearly proportional to the black hole masses; this is illustrated in Figure 1, (2)

the spectral shape changes are consistent with changes between a roughly Shakura-Sunyaev type accretion disc and an advection dominated accretion flow-like hard spectral state and (3) the phenomenon occurs at luminosities near the few percent of the Eddington limit (Ruan et al. 2019; Panda & Śniegowska 2024) where stellar mass black holes show their spectral state transitions. Having established these broad similarities between the phenomena of flip-flop transitions in black hole X-ray binaries and CLAGN, we now consider observational tests of the picture.

4.1. Searches for QPOs in CSAGN

In the X-ray binaries, the flip-flop states are often associated with the presence of low frequency (i.e. few Hz) QPOs (Buisson et al. 2025). Assuming the periods of the oscillations scale linearly with black hole mass, they should be at periods of $P \approx 2 \text{ d} \left(\frac{M_{\text{BH}}}{10^7 M_{\odot}} \right)$ in AGN.

The similarities between the spectral states indicate that these would be good places to look for QPOs in AGN. In stellar mass black holes, the amplitudes of the QPOs are seen as much higher in harder X-ray bands, dominated by the power law components (Belloni et al. 1997). For the nearest systems, observations with the Swift X-ray Telescope of about 5 ksec each are sensitive enough to detect these systems. The exposure times needed are thus quite substantial, as about 100 observations would be needed to detect the few tens of QPO cycles needed to distinguish from red noise, but this is achievable. With future instruments like NICER with better angular resolution and hence better characterised background systematics (e.g. as proposed for STROBE-X) this could be done in a significantly shorter exposure time (Ray et al. 2024). It could also be done with an imager with more collecting area than Swift, but similar responsiveness, as proposed for AXIS (Reynolds et al. 2023).

We note that one QPO has been seen in X-ray data from a CSAGN (Masterson et al. 2025). The phenomenology of this QPO does not match well to that of QPOs seen from stellar mass black holes in the past (Masterson et al. 2025). In particular, it shows characteristic frequencies that would scale to a few hundred Hz if the frequency scales linearly with the black hole mass, and shows clear evolution to higher frequencies with time.

Whether QPOs are present, but undetected in other CSAGN is unclear. The AGN in which Masterson et al. (2025) found the QPO is one of the closest CSAGN, and attracted significant attention and telescope time due to having had a major outburst. Furthermore, it has a relatively low mass black hole for an AGN. The QPO also fits within a single XMM observation's duration, rather than requiring monitoring to be detected.

The most comprehensive search for high frequency QPOs in stellar mass black holes (Belloni, Sanna, & Méndez 2012) was done (1) with power spectra averaged over full RXTE observations, so that oscillations with strong frequency evolution would change and (2) by searching only the range from 100–1 000 Hz, so that if there were a very broad excess of Fourier power around a few hundred Hz due to an oscillation changing frequency with time, it would not present a strong contrast relative to adjacent frequencies. As a result, searches for QPOs analogous to the ones seen in Masterson et al. (2025) may be warranted during the flip-flop transition states.

It is important to note that the QPO phenomenology is rather complicated for the flip-flop transitions, and not yet fully understood. Whether the QPOs are seen in the bright or the faint states

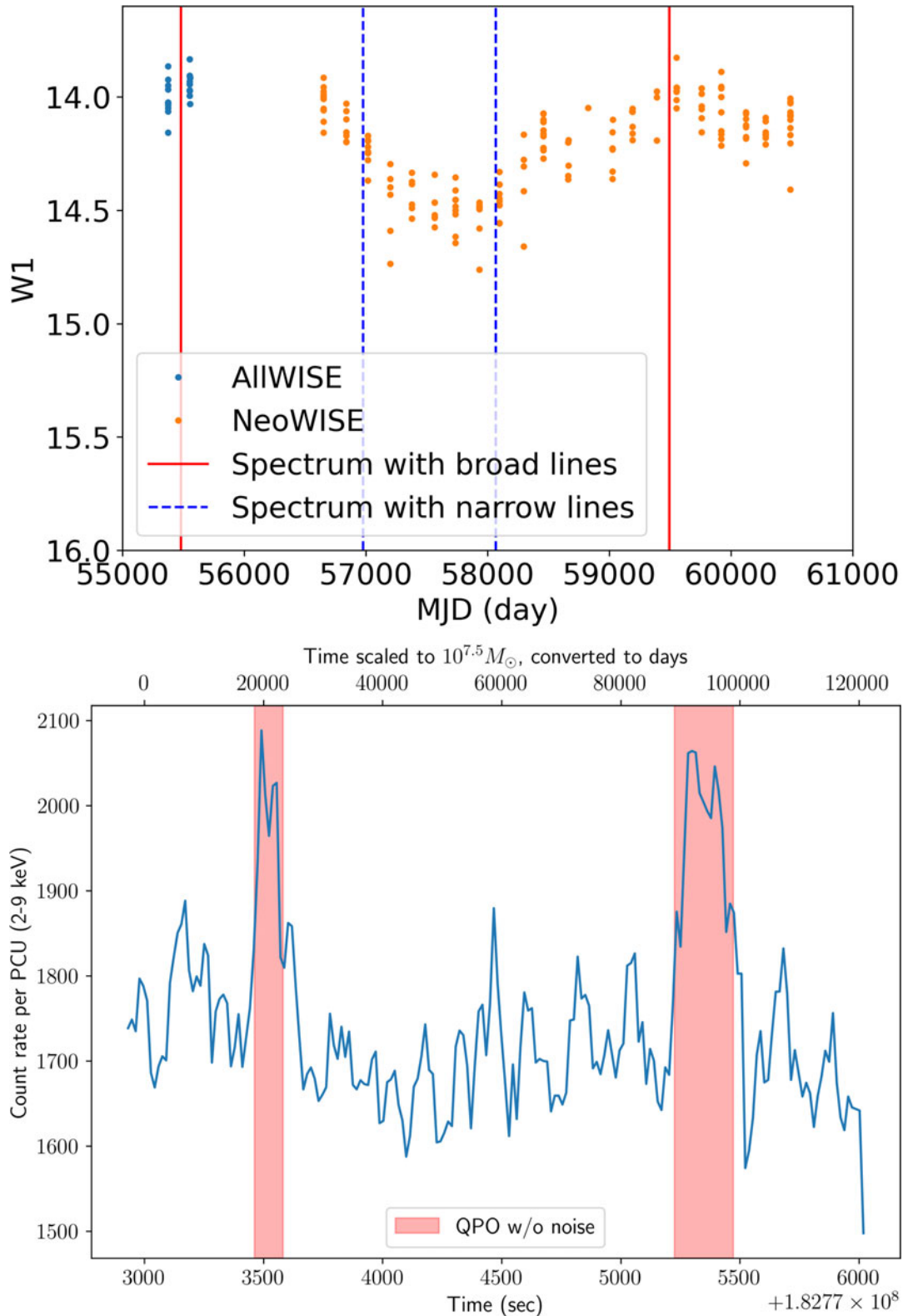


Figure 1. Top: the WISE light curve for the recurring CSAGN, J002311.06+003517.5, reported in Wang *et al.* (2025), Dong *et al.* (2025a), chosen because it shows the relevant state change and return most clearly of the recurring state change objects. For the black hole mass of approximately $10^9 M_{\odot}$, the faint state lasts the equivalent of about 3 s for a stellar mass black hole, and is one of the fastest objects in the sample of Dong *et al.* (2025a) in terms of during relative to black hole mass. Bottom: RXTE data from the source XTE J1859+226, first reported in Casella *et al.* (2004). Here, sharp changes in count rate are seen in association with changes in the Fourier power spectrum; in the fainter states, there is strong aperiodic variability and no clear QPO, while in the brighter states, there is a clear QPO and little or no aperiodic variability. The upper axis label gives the time in units re-scaled to a typical CSAGN with a black hole mass of $10^{7.5} M_{\odot}$.

varies from source to source (Bogensberger et al. 2020), and in some cases, multiple different variability patterns are seen in conjunction with the QPOs (Casella et al. 2004). At the present time, it is probably most fruitful simply to search for QPOs in the light curves of the CSAGN, and if they are found, to use them in conjunction with the properties of the QPOs from flip-flopping X-ray binaries to try to develop a real understanding of the nature of the transitions that are happening.

4.1.1. Prospects for future detections

For what we expect to see more typically (rather than what was seen in Masterson et al. 2025), QPOs on timescales of a few days, one needs sub-Nyquist sampling of the sources (i.e. observations typically about twice a day). One also needs to sample enough cycles of the oscillation to be sure that one is not seeing red noise masquerading as a QPO, a known serious problem for AGN variability (Vaughan et al. 2016). To make an estimate of the exposure time needed to detect such a phenomenon, we can look at the signal-to-noise for seeing quasi-periodic oscillations from van der Klis (2000): $n_\sigma = \frac{1}{2} I r^2 (T/\lambda)^{1/2}$, where n_σ is the signal to noise, I is the count rate, r is the rms amplitude of the oscillation, T is the exposure time and λ is the frequency width of the oscillation. We can then re-arrange this for values typical of the expectations for a supermassive black hole's QPO and solve for the needed exposure time: $T = 10^6 \text{ s} (n_\sigma/5)^2 (\lambda/10^{-6} \text{ Hz}) (r/0.03)^{-4} (I/10^{-2} \text{ cts/s})^{-2}$. The equation assumes sufficiently good sampling to resolve the QPO in time, and a sufficiently long light curve to cover the ≈ 20 cycles of the oscillation needed to ensure that the phenomenon is not red noise. Such light curves may be achievable at the present time with Swift XRT monitoring for some of the brighter objects with lower black hole masses, like NGC 4151.

It is also possible that high cadence, high sensitivity optical monitoring could detect the QPOs, but this would likely be from thermal reprocessing, rather than direct emission, and would be at lower rms amplitude (Edelson et al. 2019; Cackett, Bentz, & Kara 2021). Still, given the relative ease of obtaining high cadence optical data relative to high cadence X-ray data, this may be a practical approach to searching for QPOs. In the case of AGN, this may be possible in the optical (Smith et al. 2018). This could be done best with facilities like the Argus Array (Law et al. 2024) taking advantage of its excellent cadence.

The amplitudes of modulation that might be expected in the optical band are probably rather small, as the QPOs in the X-ray binaries show much stronger amplitudes in energy ranges dominated by non-thermal coronal emission than thermal disc emission, with strengths of the particular class of QPO (Type B) that is most often seen during flip-flop transitions of about 0.5% rms amplitude in the disc-dominated energy bands. For comparing with optical data sets, we take a re-arrangement of the QPO signal-to-noise formula where $n_\sigma = \frac{1}{2} n_{\sigma,\text{det}}^2 r^2 (\lambda T)^{-0.5}$ (Maccarone 2019), where $n_{\sigma,\text{det}}$ is the signal-to-noise for the detection of a source in the full set of observations used to make the light curve, and r is the intrinsic variability amplitude of the source (which, in background-limited data, may be much larger than the amplitude observed). T remains the actual exposure time for intermittently sampled light curves, not the duration of the time series.

We can then consider a case where a light curve of 3 months duration is produced, with about 10% duty cycle on source (yielding $T = 7.5 \times 10^5 \text{ s}$), to search for a 2-d period QPO (i.e. $5.8 \times 10^{-6} \text{ Hz}$) with frequency width of 10^{-6} Hz . We find that we need

$n_{\sigma,\text{det}} = 600 n_\sigma^{1/2} (r'/0.005)^{-1} (\lambda T/0.75)^{1/4}$ to make a QPO detection. The Argus Array should reach a magnitude of about 26 for 5σ detections^a in 3 months, while $n_{\sigma,\text{det}}$ of 600 should be reached for objects about 5 magnitudes brighter. We can then have some reasonable hope of detection optical QPOs with Argus for AGN brighter than about 21st magnitude as long as the black hole masses are in the vicinity of $10^7 M_\odot$ or smaller, but we also emphasise that this prediction is based on extrapolations that are rather uncertain. Roughly half the sky should have Argus coverage for at least three months per year. We can thus expect that essentially all of the CSAGN seen from the Sloan Digital Sky Survey (Ricci & Trakhtenbrot 2023) would be bright enough to see QPOs if our baseline assumptions are correct. Some additional work may be possible with the Vera Rubin Observatory's Legacy Survey of Space and Time (Ivezić et al. 2019), which will be able to detect objects a factor of a few fainter at the expense of cadence typically of 3 d, limiting us to searches for QPOs from AGN of more than about $10^8 M_\odot$.

Finally, as a caution, we emphasise that it is not clear that QPOs should be detectable in all of these systems, even if the same phenomenology is responsible for flip-flop transitions and CSAGN. First, there appears to be a modest inclination angle dependence for the amplitudes of different classes of QPOs (Motta et al. 2015). Second, some of the models invoked to explain the properties of QPOs require a misalignment between the black hole spin axis and the orbital plane of the binary, in order to allow for frame-dragging leading to a Lense-Thirring precession (Stella & Vietri 1998; Motta et al. 2018). Some early work suggested that large misalignments of radio jet axes from the axes of inner dust discs thought to trace the accretion disc axis were small (Kotanyi & Ekers 1979), but more recent work indicates that misalignments are likely (Schmitt et al. 2002; Ruffa et al. 2020). Alternative models can explain inclination angle dependent amplitudes without invoking misaligned discs (Varniere & Vincent 2017), and furthermore, the misalignment angles can be modest (~ 15 degrees) while still producing the QPOs (Ingram, Done, & Fragile 2009). Regardless of the potential complications, the CSAGN present excellent opportunities to search for QPOs, as they are as likely to show them as any class of AGN, and if QPOs are detected, they will be very illuminating about the nature of the changing state phenomenon.

4.2. Searches for rapid cycling of jet emission

Another core potential observational test relates to the properties of the relativistic jets. In the X-ray binaries, steady jet production is seen in hard states, but not in soft states (Tananbaum et al. 1972). The steady jets are thought to convert their bulk kinetic energy into radiation through internal shocks (Spada et al. 2001; Jamil, Fender, & Kaiser 2010).

Cross-correlations between X-ray (which comes from the accretion inflow) and infrared (which comes from the jet) light curves in GX 339-4 show a correlation coefficient of about 0.3 at their peaks, with the infrared lagging behind the X-rays by about 0.1 s (Casella et al. 2010) – the correlation is clearly statistically significant, but is also clearly not perfect. This can be explained by the internal shock model if there is a correlation between the jet speed and the X-ray luminosity (Malzac et al. 2018).

The essence of the issue here is that in the context of the internal shock model (Malzac et al. 2018), the observed *emission* from

^a<https://argus.unc.edu/specifications>.

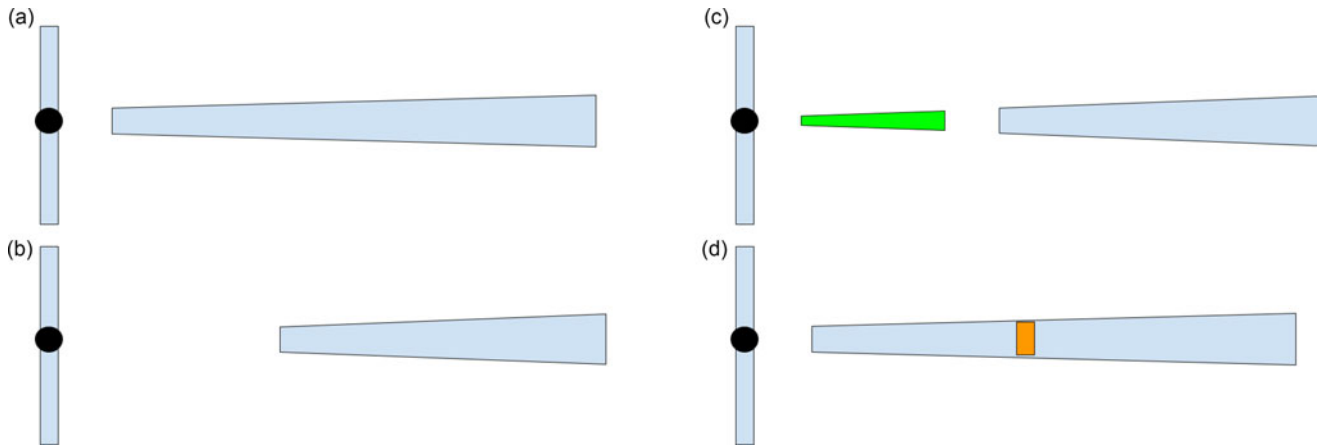


Figure 2. A cartoon illustrating the evolution of the jets in response to the state transitions. Phase (a) represents the system after it has been in a hard state for an extended period of time, and established its quasi-equilibrium configuration with stochastic variability due to internal shocks. Phase (b) represents the system after it has settled into a soft state, so that the part of the jet far from the black hole is largely unchanged, but the part near the black hole is missing. Phase (c) represents the system shortly after it re-enters a hard state, so that the new jet (in green) has started to form and has internal shocking taking place, but it has not yet re-connected with the old jet. Phase (d) represents the system shortly after the new jet reconnects with the old jet, with the orange region representing the location where the excess energy of the new jet is suddenly dissipated.

the jet on short timescales is determined by the *history* of the mass and speed of material injected into the jet. In standard hard states where this model has been tested, the X-ray variability is up to about 30% rms amplitude, with most of the variability power on timescales of seconds and faster. In flip-flop states, we can expect a rather different scenario than a steady hard state, with a lot of mass and power injected into the jet during the hard states, and little or no power injected in the soft states.

For wavelengths of light which lag the X-rays by very short timescales (such as the infrared), we can expect very little change in the observed variability properties. Starting at time τ after the state transition sets in, the properties of the previous state's jet cease to be relevant. At much longer wavelengths (such as the centimeter band), where τ exceeds the duration of the flip-flop's state change by a large factor, the effects of the flip-flopping will be smeared out to the point that they are not easily recognised. In these bands, we can expect to see somewhat weaker radio emission, because the duty cycle of the jet is reduced, and we can expect to see radio emission during both the soft and hard states, but we do not expect to see dramatic changes to the variability properties.

At intermediate wavelength, λ_{int} , for which τ has a value of a few minutes, similar to the duration of a soft or hard state during a flip-flop transition, we may expect rather dramatic changes to the jet-band light curves. In these cases, when a fast shell of material reaches the zone where photons at λ_{int} are usually emitted, in some cases there will be no matter with which to interact, because the jet has been off for a while. On the other hand, when that shell of material reaches the 'old jet' matter, it will not yet have dissipated much of its energy, so it will be moving faster, and have more energy to finally release. This will lead to stronger variability in these wavelengths. From Casella *et al.* (2010) we can see that, for X-ray binaries, the infrared lags will generally be in the low τ regime, while from Tetarenko *et al.* (2019); Tetarenko *et al.* (2021), we can see that the radio bands will generally be in the large τ regime, and the millimetre bands in the intermediate regime where extra-strong variability could be expected. For AGN with data taken in a single snapshot, this kind of behaviour would be most likely to manifest itself as a spectral energy distribution which deviates more strongly from a single power law than do the

typical spectral energy distributions of AGN in the synchrotron-dominated regime.

In Figure 2 we show a cartoon schematic of how the jet can be expected to behave through these transitions. If the system stays in the hard state for an extended period of time, it should establish a quasi-equilibrium in which its jet properties look like a steady hard state, which we illustrate in panel (a). When the transition happens, energy (and mass) injection into the inner region of the jet ceases, but the outer jet, fuelled by material ejected much earlier, will show no effects of the change, which we illustrate in panel (b). Next, in panel (c) the jet turns back on in the inner region, and the innermost and outermost parts of the jet are powered as in a steady hard state, but the intermediate region is not powered. Next, in panel (d), the two regions connect, and there is a stronger shock where they meet, as a larger-than-typical amount of power is being dissipated at that junction.

We can anticipate that in the phase corresponding to panel (a), that the jet will have its standard spectrum and brightness level for a bright hard state. In the phase corresponding to panel (b), the jet will gradually see its high frequency emission disappear, on a timescale similar to the delay time seen for propagation along the jet to the region where a particular wavelength of light is emitted. From Tetarenko *et al.* (2021), for bright, hard-state X-ray binaries, this will tend to be about $1500s(\nu/5\text{ GHz})^{-1}$.

Following Heinz & Sunyaev (2003), the break frequency at which synchrotron emission goes from optically thin to optically thick should scale with $M^{-1/3}$ under the assumptions that all the energetics of the jet behave independently of mass, and only the radiative transfer varies with mass. Given that the base height, where the jet starts having shocks energise particles will scale linearly with mass, we can expect that the time lags should then scale with mass and frequency as $1500s(\nu/5\text{ GHz})^{-1}(M/10\text{ M}_{\odot})^{2/3}$. Characteristic break frequencies are expected to be $\sim 10^{14}$ Hz in X-ray binaries and hence 10^{11-12} Hz for AGN in the $10^6-10^9\text{ M}_{\odot}$ range (Casella *et al.* 2010; Gandhi *et al.* 2011).

First, we can consider the case where we ignore the shock in panel (d), and focus on the expectations for phases (b) and (c). In an X-ray binary where the turnoff time for the jet is about 100 s, we can expect to see phenomenology in the jets related to

the flip-flop transitions for about 100 s, at frequencies above about 80 GHz. Actually measuring this would require strictly simultaneous data in either the millimetre or infrared band to go with the X-ray data to observe the flip-flops. Verifying that the jet spectrum corresponds to something like phase (c) at some point would require having at least 3 bands of long wavelength data, in addition to the X-rays, taken simultaneously. Executing this strategy would be extremely challenging to do by design, because the timing of the flip-flop transitions is unpredictable. If we take an AGN with a transition timescale of 3 yr, and a black hole mass of $10^7 M_{\odot}$, we find that the variations should be observable from about 35 GHz to the break frequency of 10^{12} Hz, precisely in the range of frequencies where CMB experiments provide wide-field monitoring data. Here, the phenomenon may even, in some cases, be observable first via jet variability.

Second, we can consider whether the shock in phase (d) can be detectable using the constraints from Fender & Bright (2019). Their equation (29) is:

$$E_m = 1.5 \times 10^{35} \text{ erg } D_{\text{kpc}}^{40/17} F_{\nu, \text{mJy}}^{20/17} \nu_{\text{GHz}}^{-23/34} \quad (3)$$

which applies for optically thick regions of the spectrum.

For this to reach about 5 mJy at 5 kpc, so that it might dominate over the steadier jet emission, we need about 10^{37} erg to be injected. This is an order of magnitude smaller than the kinetic power put into a jet launched by a 10^{37} erg/s accretion disc, with 10% jet powering efficiency, over 100 s. It is thus plausible that centimetre-band flare of order a few minutes in duration could be seen if one observed at the right time, but it may be challenging to distinguish from the stochastic jet variability that is often seen (Tetarenko et al. 2019).

If we move the distance to 100 Mpc, the energy content needed increases by a factor of about 10^{10} . We can expect energetics to scale up with M^2 (one power for the accretion rate if the Eddington fraction is fixed, and one power for the timescale), so we can then expect that even for $10^6 M_{\odot}$ black holes, such flaring would be potentially observable as a slow, optically thick transient event. This, too, is consistent with the sources seen in Nyland et al. (2020), which show very strong radio variability on decade timescales, and most of which show radio spectra which are inverted below about 10 GHz in their rest frames.

4.2.1. Searches for changing state AGN as slow radio transients

One also might expect to see transient jet behaviour in CSAGN. In fact, the transient AGN seen from the Very Large Array Sky Survey (Nyland et al. 2020) may be examples of this phenomenology, and interestingly, all the systems with good estimates of the Eddington fraction in that sample show Eddington fractions close to 10%. In the future, it may be that the best manner to discover these systems is through flaring seen by millimetre-band telescopes (Guns et al. 2021; Hervías-Caimapo et al. 2024); this would be the case both because the millimetre-band can be expected to have high-duty cycle coverage of a very wide field of view, and because the millimetre band should show more rapid variability than the longer wavelength radio band, as the emission should come from smaller regions in the jet, closer to the central black hole (Blandford & Königl 1979; Marscher & Gear 1985), something well-established to be the case for the X-ray binaries (Tetarenko et al. 2021) and for blazars (Marchili et al. 2025) and also more tentatively seen in the small fraction of systems with good radio monitoring that are unbeamed AGN (Hovatta et al. 2007; Park & Trippe 2017). Additionally, as noted above, the region of the spectrum where the

jet variability is likely to be strongest is exactly the one probed by these surveys. Follow-up with multi-epoch spectroscopy of these systems would be warranted. Similarly, radio follow-up of the optically-selected CSAGN may be fruitful, and at least one example exists of strong radio flaring correlated with a CSAGN (Meyer et al. 2025).

4.3. Searches for rapid cycling of disc winds

One of the possible analogous behaviours between X-ray binary and AGN states that has not received much attention is the phenomenology of their disc winds. Radio-loud AGN are far more likely to show double-peaked emission lines than are radio-quiet AGN (Eracleous & Halpern 2003), and this has been explained via the absence of strong winds in the radio-loud systems. In the X-ray binaries, strong disc winds are seen primarily in soft states, mainly via X-ray absorption lines (Nielsen & Lee 2009), but they can also be inferred from dipping (Díaz Trigo et al. 2006) and scattering effects (Begelman & McKee 1983).

The short durations of the faint states in the flip-flop systems, combined with the fact that they are most frequently observed with relatively low spectral resolution data, mean that searches for rapid turn-off and turn-on of disc winds in these systems has not been done (excepting the case of GRS 1915+105 Nielsen & Lee 2009, which shows some rapid state changes with a different set of characteristics than the flip-flop systems). In AGN, while this may require relatively long gratings or calorimeter observations (with facilities like Chandra or XRISM), it is straightforward to schedule searches for absorption lines in both states, and future facilities like NewAthena could be significantly more powerful in such searches (Gallo, Miller, & Costantini 2023).

5. Discussion

Previous attempts to draw analogies between CSAGN and X-ray binaries have focused on the ‘standard’ state transitions, which tend to happen on month timescales in X-ray binaries, and hence would be unobservable in AGN if their timescales scaled linearly with black hole mass – see Table 1. Here we have shown that by associating the CSAGN instead with flip-flop states, we can reconcile the timescales for the changing-state effect very well. While direct evidence linking the two phenomena remains limited, we discuss numerous new observations that could provide stronger connections. Attacking the problem using both sets of data could help substantially. Furthermore, the finding that both stellar mass black holes and AGN show essentially the same phenomenology for rapid spectral transitions argues against models in which a mechanism is invoked that is particular to one class of system (e.g. through tidal disruptions – Wang et al. 2024 or through the radiation pressure instability as mentioned in Buisson et al. 2025).

A plausible mechanism for making the timescales so fast is to invoke the thermal timescale. Near the critical accretion rate for the state transition, gas may be thermally unstable in the accretion disc (Takizawa et al. 1997). The thermal timescale for accretion discs is typically $t_{\text{th}} = \frac{1}{\alpha\Omega}$. Thus, if α is similar for AGN and X-ray binaries, the timescale for changes should scale approximately linearly with black hole mass.

There are two potential strong tests of this picture. One is that CSAGN are excellent candidates for showing QPOs, with characteristic timescales of a few days to a few months. Monitoring observations of these systems should be done with sufficient sensitivity

and cadence to search for these oscillations. The second is that in both classes of systems, the jet behaviour should be anomalous. Understanding this may be easier with radio or millimetre-band searches for transient AGN than in X-ray binaries as the X-ray binary phenomena happen very quickly and unpredictably, meaning one would need to be lucky about when multi-wavelength data were scheduled.

Acknowledgments. Several of us thank Gullo Mastroserio for organising a workshop in Milan where the seeds for this work were planted. TJM thanks Vanderbilt University, and especially Manuel Pichardo Marcano, for hospitality during a visit in which the idea truly jelled, and Megan Masterson for useful discussions about AGN QPOs and Doug Lin for discussions about the possibility that CSAGN are driven by tidal disruptions. GM acknowledges financial support from the Academy of Finland grant 355672. This research was supported in part by grant NSF PHY-2309135 to the Kavli Institute for Theoretical Physics (KITP). We thank both the anonymous referee and the editor for comments which have improved the quality of this manuscript.

References

- Begelman, M. C., & McKee, C. F. 1983, *ApJ*, **271**, 89
- Belloni, T., van der Klis, M., Lewin, W. H. G., van Paradijs, J., Dotani, T., Mitsuda, K., & Miyamoto, S. 1997, *A&A*, **322**, 857
- Belloni, T. M., Sanna, A., & Méndez, M. 2012, *MNRAS*, **426**, 1701
- Blandford, R. D., & Königl, A. 1979, *ApJ*, **232**, 34
- Bogensberger, D., et al. 2020, *A&A*, **641**, A101
- Buisson, D. J. K., Marcel, G., López-Barquero, V., Motta, S. E., Turner, S. G. D., & Vincentelli, F. M. 2025, arXiv e-prints, art. arXiv: 2502.08718
- Cackett, E. M., Bentz, M. C., & Kara, E. 2021, *ISci*, **24**, 102557
- Casella, P., Belloni, T., Homan, J., & Stella, L. 2004, *A&A*, **426**, 587
- Casella, P., et al. 2010, *MNRAS*, **404**, L21
- Díaz Trigo, M., Parmar, A. N., Boirin, L., Méndez, M., & Kaastra, J. S. 2006, *A&A*, **445**, 179
- Dong, Q., Zhang, Z.-X., Gu, W.-M., Sun, M., Guo, W.-J., Cai, Z.-Y., Wang, J.-X., & Zheng, Y.-G. 2025a, arXiv e-prints, art. arXiv: 2510.18445
- Dong, Q., Zhang, Z.-X., Gu, W.-M., Sun, M., & Zheng, Y.-G. 2025b, *ApJ*, **986**, 160
- Duffy, L., Eracleous, M., Ruan, J. J., Yang, Q., & Runnoe, J. C. 2025a, arXiv e-prints, art. arXiv: 2504.06065
- Duffy, L., Eracleous, M., Runnoe, J. C., Ruan, J. J., Anderson, S. F., Dimassimo, S., Green, P., & LaMassa, S. 2025b, *ApJ*, **981**, 127
- Dunn, T., et al. 2025, arXiv e-prints, art. arXiv: 2510.25156
- Edelson, R., et al. 2019, *ApJ*, **870**, 123
- Eracleous, M., & Halpern, J. P. 2003, *ApJ*, **599**, 886
- Fabian, A. C. 2012, *ARA&A*, **50**, 455
- Fender, R., & Bright, J. 2019, *MNRAS*, **489**, 4836
- Fryer, C. L., Belczynski, K., Wiktorowicz, G., Dominik, M., Kalogera, V., & Holz, D. E. 2012, *ApJ*, **749**, 91
- Gallo, E., Fender, R. P., & Pooley, G. G. 2003, *MNRAS*, **344**, 60
- Gallo, L. C., Miller, J. M., & Costantini, E. 2023, in *High-Resolution X-ray Spectroscopy: Instrumentation*, ed. C. Bambi, & J. Jiang, 209. doi:10.1007/978-981-99-4409-5 9
- Gandhi, P., et al. 2011, *ApJ*, **740**, L13
- Guns, S., et al. 2021, *ApJ*, **916**, 98
- Hannikainen, D. C., Hunstead, R. W., Campbell-Wilson, D., & Sood, R. K. 1998, *A&A*, **337**, 460
- Heinz, S., & Sunyaev, R. 2002, *A&A*, **390**, 751
- Heinz, S., & Sunyaev, R. A. 2003, *MNRAS*, **343**, L59
- Hervías-Caimapo, C., et al. 2024, *MNRAS*, **529**, 3020
- Ho, L. C. 1999, *ApJ*, **516**, 672
- Homan, J., Wijnanders, R., van der Klis, M., Belloni, T., van Paradijs, J., Klein-Wolt, M., Fender, R., & Méndez, M. 2001, *ApJS*, **132**, 377
- Hovatta, T., Tornikoski, M., Lainela, M., Lehto, H. J., Valtaoja, E., Tornainen, I., Aller, M. F., & Aller, H. D. 2007, *A&A*, **469**, 899
- IceCube Collaboration, et al. 2018, *Sci*, **361**, eaat1378
- Ingram, A., Done, C., & Fragile, P. C. 2009, *MNRAS*, **397**, L101
- Ivezić, Ž., et al. 2019, *ApJ*, **873**, 111
- Jamil, O., Fender, R. P., & Kaiser, C. R. 2010, *MNRAS*, **401**, 394
- Koljonen, K. I. I., Satalecka, K., Lindfors, E. J., & Lioudakis, I. 2023, *MNRAS*, **524**, L89
- Komossa, S., & Grupe, D. 2024, *SerAJ*, **209**, 1–24
- Körding, E. G., Jester, S., & Fender, R. 2006, *MNRAS*, **372**, 1366
- Kotanyi, C. G., & Ekers, R. D. 1979, *A&A*, **73**, L1–L3
- Law, et al. 2024, in *American Astronomical Society Meeting Abstracts*, Vol. 243, American Astronomical Society Meeting Abstracts, 237.06
- Maccarone, T. J. 2003, *A&A*, **409**, 697
- Maccarone, T. J. 2019, *RNAAS*, **3**, 116
- Maccarone, T. J., & Coppi, P. S. 2003, *MNRAS*, **338**, 189
- Maccarone, T. J., Gallo, E., & Fender, R. 2003, *MNRAS*, **345**, L19
- Maccarone, T. J., Osler, A., Miller-Jones, J. C. A., Atri, P., Russell, D. M., Meier, D. L., McHardy, I. M., & Longa-Peña, P. A. 2020, *MNRAS*, **498**, L40
- Malzac, J., et al. 2018, *MNRAS*, **480**, 2054
- Marchili, N., et al. 2025, *A&A*, **702**, A140
- Marscher, A. P., & Gear, W. K. 1985, *ApJ*, **298**, 114
- Masterson, M., et al. 2025, *Natur*, **638**, 370
- McHardy, I. M., Koerding, E., Knigge, C., Uttley, P., & Fender, R. P. 2006, *Natur*, **444**, 730
- Merloni, A., Heinz, S., & di Matteo, T. 2003, *MNRAS*, **345**, 1057
- Meyer, E. T., et al. 2025, *ApJ*, **979**, L2
- Miyamoto, S., Kimura, K., Kitamoto, S., Dotani, T., & Ebisawa, K. 1991, *ApJ*, **383**, 784
- Moravec, E., Svoboda, J., Borkar, A., Boorman, P., Kynoch, D., Panessa, F., Mingo, B., & Guainazzi, M. 2022, *A&A*, **662**, A28
- Motch, C., Ricketts, M. J., Page, C. G., Ilovaisky, S. A., & Chevalier, C. 1983, *A&A*, **119**, 171
- Motta, S. E., Casella, P., Henze, M., Muñoz-Darias, T., Sanna, A., Fender, R., & Belloni, T. 2015, *MNRAS*, **447**, 2059
- Motta, S. E., Franchini, A., Lodato, G., & Mastroserio, G. 2018, *MNRAS*, **473**, 431
- Neilsen, J., & Lee, J. C. 2009, *Natur*, **458**, 481
- Noda, H., & Done, C. 2018, *MNRAS*, **480**, 3898
- Nyland, K., et al. 2020, *ApJ*, **905**, 74
- Panda, S., & Śniegowska, M. 2024, *ApJS*, **272**, 13
- Park, J., & Trippie, S. 2017, *ApJ*, **834**, 157
- Pierre Auger Collaboration, et al. 2007, *Sci*, **318**, 938
- Punch, M., et al. 1992, *Natur*, **358**, 477
- Ray, P. S., et al. 2024, *JATIS*, **10**, 042504
- Reynolds, C. S., et al. 2023, in *UV, X-Ray, and Gamma-Ray Space Instrumentation for Astronomy XXIII*, Vol. 12678, *Society of Photo-Optical Instrumentation Engineers (SPIE) Conference Series*, ed. O. H. Siegmund, & K. Hoadley, 126781E. doi:10.1117/12.2677468
- Ricci, C., & Trakhtenbrot, B. 2023, *NatAs*, **7**, 1282
- Ruan, J. J., Anderson, S. F., Eracleous, M., Green, P. J., Haggard, D., MacLeod, C. L., Runnoe, J. C., & Sobolewska, M. A. 2019, *ApJ*, **883**, 76
- Ruffa, I., Laing, R. A., Prandoni, I., Paladino, R., Parma, P., Davis, T. A., & Bureau, M. 2020, *MNRAS*, **499**, 5719
- Rumbaugh, N., et al. 2018, *ApJ*, **854**, 160
- Schmitt, H. R., Pringle, J. E., Clarke, C. J., & Kinney, A. L. 2002, *ApJ*, **575**, 150
- Smith, K. L., Mushotzky, R. F., Boyd, P. T., & Wagoner, R. V. 2018, *ApJ*, **860**, L10
- Śniegowska, M., Czerny, B., Bon, E., & Bon, N. 2020, *A&A*, **641**, A167
- Sobolewska, M. A., Siemiginowska, A., & Gierliński, M. 2011, *MNRAS*, **413**, 2259
- Spada, M., Ghisellini, G., Lazzati, D., & Celotti, A. 2001, *MNRAS*, **325**, 1559
- Stella, L., & Vietri, M. 1998, *ApJ*, **492**, L59
- Takizawa, M., et al. 1997, *ApJ*, **489**, 272
- Tananbaum, H., Gursky, H., Kellogg, E., Giacconi, R., & Jones, C. 1972, *ApJ*, **177**, L5
- Tavani, M., et al. 2009, *Natur*, **462**, 620
- Tetarenko, A. J., Casella, P., Miller-Jones, J. C. A., Sivakoff, G. R., Tetarenko, B. E., Maccarone, T. J., Gandhi, P., & Eikenberry, S. 2019, *MNRAS*, **484**, 2987

- Tetarenko, A. J., et al. 2021, *MNRAS*, **504**, 3862
Trichas, M., et al. 2013, *ApJ*, **778**, 188
Vahdat Motlagh, A., Kalemci, E., & Maccarone, T. J. 2019, *MNRAS*, **485**, 2744
van der Klis, M. 1994, *ApJS*, **92**, 511
van der Klis, M. 2000, *ARA&A*, **38**, 717
Varniere, P., & Vincent, F. H. 2017, *ApJ*, **834**, 188
- Vaughan, S., Uttley, P., Markowitz, A. G., Huppenkothen, D., Middleton, M. J., Alston, W. N., Scargle, J. D., & Farr, W. M. 2016, *MNRAS*, **461**, 3145
Wang, S., Woo, J.-H., Gallo, E., Son, D., Yang, Q., Jin, J., Guo, H., & Kong, M. 2025, *ApJ*, **981**, 129
Wang, Y., Lin, D. N. C., Zhang, B., & Zhu, Z. 2024, *ApJ*, **962**, L7
Zhang, S. N., Cui, W., & Chen, W. 1997, *ApJ*, **482**, L155